OXFORD
UNIVERSITY PRESS

Archives of Clinical Neuropsychology 27 (2012) 915–929

Archives of CLINICAL NEUROPSYCHOLOGY

Evidence of Change in Brain Activity among Childhood Cancer Survivors Participating in a Cognitive Remediation Program

Ping Zou[1], Yimei Li[2], Heather M. Conklin[3], Raymond K. Mulhern[3]†, Robert W. Butler[4], Robert J. Ogg[1,*]

[1]*Department of Radiological Sciences, St. Jude Children's Research Hospital, Memphis, TN, USA*
[2]*Department of Biostatistics, St. Jude Children's Research Hospital, Memphis, TN, USA*
[3]*Department of Psychology, St. Jude Children's Research Hospital, Memphis, TN, USA*
[4]*Department of Psychiatry, Oregon Healthy & Science University, Memphis, TN, USA*

*Corresponding author at: Department of Radiological Sciences, St. Jude Children's Research Hospital, 262 Danny Thomas Pl., Memphis, TN 38105, USA. Tel.: +901-595-2412; fax: +901-595-3981.
E-mail address: robert.ogg@stjude.org (R. J. Ogg).

Accepted 25 September 2012

Abstract

Increased understanding of the underlying mechanisms of cognitive remediation is needed to facilitate development of intervention strategies for childhood cancer survivors experiencing cognitive late effects. Accordingly, a pilot functional magnetic resonance imaging (fMRI) study was conducted with 14 cancer survivors (12.02 ± 0.09 years old), who participated in a cognitive remediation clinical trial, and 28 healthy children (12.7 ± 0.6 years old). The ventral visual areas, cerebellum, supplementary motor area, and left inferior frontal cortex were significantly activated in the healthy participants during a continuous performance task. In survivors, brain activation in these regions was diminished at baseline, and increased upon completion of remediation and at a 6-month follow-up. The fMRI activation index for each region of interest was inversely associated with the Conners' Clinical Competence Index ($p < .01$). The pilot study suggests that fMRI is useful in evaluating neural responses to cognitive remediation.

Keywords: Attention; Brain tumor; Childhood brain insult; Neuroimaging (functional); Rehabilitation

Introduction

Acute lymphoblastic leukemia (ALL) and brain tumor are the two most common forms of childhood cancers, accounting for more than 50% of all childhood cancer (American Cancer Society, 2011). Cognitive deficits in long-term survivors of childhood ALL or brain tumors are well documented and progressively worsen over the years, affecting attention, processing speed, working memory, executive functions, intelligence, and academic skills (Brouwers, Riccardi, Poplack, & Fedio, 1984; Brouwers & Poplack, 1990; Mulhern, Merchant, Gajjar, Reddick, & Kun, 2004; Palmer, Reddick, & Gajjar, 2007). Although ALL and brain tumor are very different diseases, their survivors develop similar patterns of cognitive deficits; these long-term cognitive deficits have primarily been associated with cancer therapies directed at the central nervous system (CNS) (Butler & Haser, 2006). CNS prophylactic therapy, including cranial irradiation, intrathecal chemotherapy, or both, is used in patients with ALL to prevent relapses in the CNS. For many patients with brain tumors, cranial radiation and chemotherapy are essential parts of curative therapy (Conklin, Li, Xiong, Ogg, & Merchant, 2008; Merchant, Happersett, Finlay, & Leibel, 1999; Merchant, Conklin, Wu, Lustig, & Xiong, 2009).

With modern therapy, 5-year survival rates for leukemia and CNS cancers have reached 82% and 71%, respectively (American Cancer Society, 2011). As the population of cancer survivors increases, strategies to alleviate the negative

† Deceased.

doi:10.1093/arclin/acs095 Advance Access publication on 18 October 2012

effects of cognitive deficits in survivors' lives are urgently needed. The neural basis of the cognitive deficits in ALL and brain tumor survivors must be understood to minimize cognitive sequelae of therapies directed to the CNS and to guide the design and evaluation of future cognitive interventions for these survivors. Neuroimaging plays an increasingly important role not only in the diagnosis and treatment of cancer but also in understanding the late cognitive effects in these patients. Conventional brain imaging has revealed anatomic abnormalities, particularly white matter differences, in the brains of survivors of childhood ALL and brain tumors (Carey et al., 2008; Reddick et al., 2000; Reddick, Glass, Johnson, Laningham, & Pui, 2009; Zhang et al., 2008). These abnormalities have been associated with declining IQ, academic struggles, difficulties in acquiring new knowledge, and problems with attention (Mulhern et al., 2001, 2004; Palmer et al., 2001, 2007). However, the neural substrates underlying cognitive sequelae in the survivors of childhood ALL and brain tumors are unknown.

Functional magnetic resonance imaging (fMRI) measures brain activation patterns through local hemodynamic responses during sensory, motor, or cognitive tasks. This non-invasive technique offers new opportunities to understand cognitive deficits in cancer survivors. A study with simple visual stimulation during fMRI demonstrated that blood oxygenation level-dependent (BOLD) fMRI, the most commonly used fMRI method, is feasible in childhood survivors of ALL and brain tumor (Zou, Mulhern, et al., 2005), and that the BOLD signal mechanism was largely intact. However, the BOLD responses to simple visual stimulation were altered during the course of treatment (cranial radiation and chemotherapy) in pediatric brain tumor patients and were associated with reaction time (Zou, Philips, et al., 2005). Survivors of childhood ALL showed increased activation in prefrontal cortices in an fMRI working memory study, and activation patterns were consistent with the theory of compensatory activation of related brain regions (Robinson et al., 2010). Thus, fMRI is sensitive to changes in brain function in pediatric cancer survivors and may be useful to investigate cognitive remediation in these children.

Multiple behavioral and pharmacologic intervention trials have been conducted to treat attention and cognitive deficits among childhood cancer survivors (Butler & Copeland, 2002; Butler et al., 2008; Conklin et al., 2007; Thompson et al., 2001). These interventions yielded promising results; however, long-term benefits of remediation are unknown. A pilot study with pediatric cancer survivors (Butler & Copeland, 2002) showed improved performance on a standard test of attention (Conner's Continuous Performance Task [CPT]) after a cognitive remediation program (CRP). A subsequent randomized controlled clinical trial of CRP with pediatric cancer survivors at seven sites nationwide (Butler et al., 2008) showed improved attention by parent report and increased academic achievement, but no CPT improvement related to CRP. During the CRP clinical trial (Butler et al., 2008), optional fMRI examinations were offered to CRP participants at one of the seven sites to investigate brain activation patterns. The goal of the pilot fMRI study was to characterize the effects of cognitive remediation on the brain's functional networks. We report here findings from the fMRI examinations conducted at baseline, upon CRP completion, and at a follow-up 6 months after CRP completion.

Method

Participants

This fMRI study was conducted as a pilot study embedded in a multi-site, randomized, controlled, clinical trial of CRP in childhood cancer survivors (Butler et al., 2008); the fMRI data were collected at one of the participating sites during the clinical trial. The fMRI study was approved by the Institutional Review Board, and written informed consent, with assent from the patient as appropriate, was obtained from each patient's parent or guardian prior to participation. To be eligible for the CRP clinical trial, patients had to meet the following criteria: age 6–17 years (inclusive); English-speaking; enrolled in school or homebound instruction; diagnosis of leukemia, lymphoma, or brain tumor; disease remission and off treatment at least 1 year; no history of CNS involvement predating cancer; no history of documented attention-deficit disorder or learning disability predating cancer; had not been treated with psychostimulants or psychotropic medications intended to treat mood or thought disorders for at least 2 weeks; not living more than 80 km from the hospital; and no major physical, neurologic, or psychiatric condition that would preclude participation in the research program. Finally, the CRP participants needed to show attention deficits at baseline screening documented as: (i) Clinical Competence Index (CCI) $\geq$60 on Conners' CPT or (ii) CCI from 50 to 59 on Conners' CPT and T-score $\geq$60 on Conners' Parent Rating Cognitive Problems/Inattentive Scale.

Of the 20 eligible participants, 12 were randomly assigned to the treatment group and 8 were assigned to the standard-of-care wait-list control group. Of the 20 eligible CRP participants, 14 had fMRI examinations at least one time (Table 1). Psychologic evaluations and fMRI examinations occurred at three time points: pre-CRP (baseline); post-CRP (upon completion of CRP); and follow-up (6 months after completion of CRP). The survivors in the wait-list control group were offered the chance to participate in CRP 6 months after baseline and to receive optional fMRI examinations after completing their CRP sessions. In addition, psychologic evaluation and fMRI examination were conducted once in 28 age-matched

Table 1. Cancer survivors participating in fMRI examinations

Group	Sex	Age at DX (years)	Age at the first fMRI (years)	DX	IQ	CPT CCI			Functional MRI		
						Pre-CRP	Post-CRP or Pre-CRP +6 month	Follow-up	Pre-CRP	Post-CRP	Follow-up
CRP	F	4.3	15.0	ALL	92	51.8	49.9	59.9	Y	Y	Y
CRP	F	2.8	11.7	ALL	70	61.1	16.2	0.1	Y	Y	Y
CRP	F	1.9	7.8	ALL	81	52.2	44.1	40.4	Y	—	Y
CRP	F	12.6	15.2	ALL	75	99.9	71.3	69.5	X	X	X
CRP	F	3.5	8.7	ALL	77	69.2	43.4	53	Y	—	Y
CRP	M	7.9	16.9	BT[a]	95	65.3	48.5	58.6	—	Y	Y
CRP	M	6.9	14.6	BT[b]	69	60.2	73.1	71.6	Y	—	Y
CRP	F	8.0	17.0	BT[c]	60	81.4	84.4	62.4	—	X	X
Wait-list	M	2.0	9.8	ALL	101	58.9	65.6	[f]	Y	Y*	[f]
Wait-list	F	7.1	11.3	ALL	97	74.2	78.6	[f]	Y	Y*	[f]
Wait-list	F	2.9	9.5	BT[b]	99	62.2	49.9	[f]	Y(2)	Y*	[f]
Wait-list	F	10.8	15.1	BT[d]	89	53	55.9	[f]	X	X*	[f]
Wait-list	F	7.3	10.5	BT[d]	80	63.3	53.8	[f]	Y(2)	—	[f]
Wait-list	M	4.7	6.6	BT[e]	107	58.1	32.2	[f]	X	—	[f]

Note: Diagnosis (DX) for the cancer survivors included acute lymphoblastic leukemia (ALL) and brain tumor. The total 14 survivors (8 CRP and 6 initial wait-list controls) had fMRI during at least one timepoint: "Y" indicates data acquired, and "X" indicates those patients whose image data were excluded from the second-level analysis because of normalization problems with brain lesions or brain images that were distorted due to shunts or braces; "—" indicates missing fMRI at the time point; "*" indicates fMRIs for initial wait-list survivors at their completion of CRP; "(2)" indicates 2 fMRIs (6-month apart) for the initial wait-list survivors before they received CRP.

[a]BT = ependymoma.

[b]BT = astrocytoma.

[c]BT = suprasellar germinoma.

[d]BT = medulloblastoma.

[e]BT = suprasella craniopharyngioma.

[f]No clinical CPT data were collected at the follow-up time point for the wait-list group.

healthy children (12.7 ± 0.6 years old; 15 girls and 13 boys). These healthy children met all CRP eligibility criteria, except that they were cancer free and without documented attention deficits.

CRP and Psychologic Evaluation

The CRP is based on a tripartite model that combines interventions derived from brain injury rehabilitation (e.g., massed practice), educational psychology (e.g., instruction in metacognitive strategies, such as task preparedness and monitoring), and child clinical psychology [e.g., cognitive behavioral strategies including monitoring of internal dialogues and reframing of cognitive struggles (Butler & Copeland, 2002)]. CRP was individually administered by a therapist who was a graduate-level clinical psychology student, equivalent healthcare professional, or postdoctoral fellow. Participants in the CRP were trained during about 20 sessions (2 h per session per week) over 4–5 months (Butler et al., 2008). Specific CRP interventions were programmatic yet individualized based on the participants' abilities and needs. To ensure treatment integrity, regular conference calls with site principal investigators and research assistants were conducted. Therapists also submitted training videotapes demonstrating in vivo competence to the two principal investigators throughout the course of the study.

Academic achievement, neuropsychologic, and objective psychologic measures for participants included: Conners' CPT-II (Conners, 1992), Wide Range Achievement Test—Third Edition (Wilkinson, 1993), Woodcock–Johnson Tests of Achievement—Revised (Woodcock & Johnson, 1989), Peabody Individual Achievement Test—Revised (Dunn & Markwardt, 1970), Wechsler Intelligence Scale for Children—Third Edition (WISC-III; Wechsler, 1991), Wide Range Achievement Test of Memory and Learning (Sheslow & Adams, 1990), Children's Memory Scale (Cohen, 1997), Rey Auditory Verbal Learning Test Trial 1 (Rey, 1964), Stroop Color–Word Test Trial 3 (Golden, 1978), Trail Making Test Part B (Reitan, 1969), Brief Test of Attention (Schretlen, 1997), Rey–Osterrieth Complex Figure Test (Lezak, Howieson, & Loring, 2004) Conners' Parent Rating Scale: Long Version—Revised (CPRS: LV-R, Conners, 1997), Conners' Teacher Rating Scale: Long Version—Revised (CTRS: LV-R; Conners,1997), and Culture-Free Self-Esteem Inventory—Second Edition (Battle, 1992).

The CCI of Conners' CPT was used as a primary behavioral endpoint to evaluate the efficacy of CRP in the clinical trial. CCI is computed to discriminate attention deficit hyperactivity disorder (ADHD) from the general population in the presumed

real world. While the CCI has flawed properties from a statistical standpoint (e.g., it is not an index that is scaled on traditional interval based metrics), it does provide a measure that has greater clinical import in everyday functioning than the individual indices that comprise its makeup. Test–retest reliability for the CCI is high (0.84) and comparisons of nonclinical control participants and individuals diagnosed with attentional difficulties have reported statistically significant differences (Analysis of Covariance, $p < .001$) on this index (Conners, 1992).

FMRI Paradigm

CPT was chosen as a task for the exploratory fMRI study during the CRP clinical trial because activation during the fMRI CPT included brain regions involved in visual object processing, motor control, and attentional control (Ogg et al., 2008)—an extensive neural network that might be affected by the CRP treatment. Furthermore, the CPT CCI, which is affected by a wide range of brain functions, can be analyzed in relation to the fMRI results.

Based on the observations that cancer survivors may have different hemodynamic responses to neural activity, which may reduce sensitivity in detecting brain activation with BOLD fMRI (Zou, Mulhern, et al., 2005), the fMRI CPT was presented in a block-wise paradigm (Ogg et al., 2008) to facilitate the detection of activation (Liu, 2004). The CPT fMRI paradigm included six blocks, each consisting of 20 s of task and 20 s of rest. During the task condition, 20 letters, 2 of which were the target letter "X," were presented in a random order. Each letter was projected on the screen for 250 ms, and the interval between the letters was 1 s. Participants were instructed to push a button when presented with a letter except the target letter "X." During the rest condition, they were instructed to maintain their gaze on a small fixation cross projected in the center of the gray screen.

FMRI Data Acquisition and Analysis

Functional MRI was performed using a 1.5 T Siemens Symphony scanner with the standard quadrature headcoil. A single-shot T_2*-weighted echo planar imaging pulse sequence (TR = 2.06 s, TE = 50 ms, FOV = 192 mm, matrix = 64 × 64, slice thickness = 5 mm, 23 slices, and bandwidth = 1954 Hz/pixel) was used to acquire the functional images of the whole brain. A total of 125 image volumes were acquired per run for the CPT task, with the first 5 volumes being discarded to allow for T_1 equilibration effects.

Image analysis was conducted with the statistical parametric mapping (SPM) software program SPM2 (Wellcome Trust Centre for Neuroimaging, London, UK). Preprocessing of functional images included realignment to correct for head motion during scanning and normalization to a standard echo planar imaging brain template in MNI (Montreal Neurological Institute) space with a resampled isotropic voxel size of 2 mm. The normalized images were smoothed with a Gaussian kernel of 6-mm full width at half maximum (FWHM). Each participant's preprocessed images were analyzed using the general linear model based on the block-wise design of the fMRI CPT task paradigm. After parameter estimation of the general linear model, contrasts reflecting greater activation during the task period than during the fixation period (i.e., CPT > fixation) or greater activation during the fixation period than during the task period (i.e., fixation > CPT) were set, and two contrast images from each subject were generated. Contrast images were then used as variables in second-level random-effect analyses to identify group patterns of brain activation and activation differences both between groups and at different time points. Additionally, each participant's CPT CCI from the standard test (Conners, 1992) and performance measures during fMRI (omission errors, commission errors, and reaction times) were used as covariates in the second-level analysis to identify associated activation regions. A cluster-based statistical threshold was used to identify activated brain regions: voxel height $T = 5$ (uncorrected $p < .001$, family-wise corrected $p = .48$) and extent $k = 50$ voxels (uncorrected $p = .002$, corrected $p = .001$). Activated clusters were automatically labeled by using the AAL (Anatomical Automatic Labeling) toolbox (Tzourio-Mazoyer et al., 2002) and checked visually against anatomical atlases (Schmahmann et al., 1999; Talairach & Tournoux, 1998).

Region of Interest (ROI) Analysis

To further characterize the clinical relevance of brain activation patterns, ROI analysis was conducted. ROIs were the activation regions from the healthy control's activation map at thresholds $T = 5$ and cluster size >50 voxels. Each participant's activation index (AI) was calculated from the SPM T-map by adding the t values of all the voxels that were thresholded at $t > 2$ in an activation ROI or by adding the t values of all the voxels that were thresholded at $t < -2$ in a deactivation ROI. This definition of AI is similar to that used in a previous n-back working memory fMRI study (Wei et al., 2004). It combines the effects of BOLD signal strength and activation volume, both of which are relevant to possible changes in neural-hemodynamic coupling and neural recruitment in response to cancer, cancer treatment directed at the CNS, and cognitive

remediation. Finally, the normalized AI (nAI) was defined as the scaled activation score for which the average score was 1 for the ROI in healthy control participants. Laterality index (LI), defined as $LI = (nAI_{left} - nAI_{right})/(nAI_{left} + nAI_{right})$, was calculated for bilateral ROIs. Spearman correlation analyses were performed between the nAI and each group's CPT CCI at each time and each region separately. The nAIs of the groups at each time point were compared using the Wilcoxon rank-sum test. Finally, the within-group nAI changes across the time points in survivors were analyzed using the Wilcoxon signed-rank test. All statistical analyses were performed with SAS 9.2 software (SAS institute, Cary, NC).

Results

Neuropsychologic Evaluation

Compared with healthy controls, cancer survivors performed significantly worse on a measure of intellectual functioning, with Wechsler Intelligence Scale for Children (WISC-III; Wechsler, 1991) FSIQ values of 101.8 ± 2.6 and 85.2 ± 4.4 (at screening phase), respectively. At pre-CRP, the average CCI of the survivors was significantly greater than that of the healthy controls (63.8 ± 3.8 vs. 43.8 ± 3.1, $p < .001$, effect size Cohen's $d = -1.4$), but there was no significant difference between the CPT CCIs of the survivors in the CRP treatment and wait-list control groups (65.4 ± 6.5 vs. 61.6 ± 2.6, $d = 0.3$). The CRP group's CCI significantly decreased after CRP (65.4 ± 6.5 vs. 53.9 ± 7.6, $p = .036$, $d = -0.6$); further, the CRP group's CCIs were similar at post-CRP and at follow-up. In contrast, there was no significant change in the CPT CCI for the wait-list control group (Table 1).

The Conners' Parent Rating Scale (CPRS: LV-R, Conners, 1997) T-scores for both survivor groups were abnormal (>60) or nearly abnormal for the three scales: Cognitive Problems/Inattention, Hyperactivity, and ADHD at any given timepoint (Table 2). The *T*-scores were not significantly different between the CRP and the wait-list groups at baseline and at the second timepoint for each of the three scales. Both groups improved on the areas of Cognitive Problems/Inattention and ADHD between the first and the second timepoint. The improvements for the CRP group were significant between baseline and the 6-month follow-up in Cognitive Problems/Inattention (*T* scores: 72.6 ± 5.1 vs. 63.6 ± 5.6, $p = .02$, $d = -0.6$) and in ADHD (*T* scores: 67.0 ± 3.4 vs. 59.5 ± 5.4, $p = .04$, $d = -0.6$).

Neuroimaging Examination

The fMRI data were acquired from 14 survivors (8 CRP and 6 initial wait-list controls) during at least one timepoint (Table 1): pre-CRP (6 CRP and 6 initial wait-list controls); post-CRP (6 CRP and 4 initial wait-list controls); and follow-up (6 CRP). However, fMRI images of four survivors were excluded from second-level analysis because of incompatible normalization with brain lesions or image distortion due to shunts or braces. Compared with healthy controls, survivors had more omission errors (3.5 ± 1.0 vs. 1.5 ± 0.4, $p = .04$, $d = -0.6$), a similar number of commission errors (5.1 ± 0.9 vs. 5.3 ± 0.7, $p = .8$, $d = 0.05$), and slower reaction time (388 ± 21 vs. 342 ± 15 ms, $p = .09$, $d = -0.6$) during the fMRI CPT task.

With the cluster-level threshold, significant brain activation during the CPT task periods and "deactivation" during the resting periods were detected in the healthy controls (Table 3) and survivors (Table 4) at three timepoints (Fig. 1). In survivors at pre-CRP, activation regions identified in healthy children, such as in the cerebellum_crus 1, cerebellum_area 6, inferior occipital, fusiform, and insula, were not activated; and the more anterior region of cingulate and supplementary motor areas (SMAs) were activated. Survivors' "deactivation" regions involved more calcarine areas, fewer precuneus areas, and a small right precentral area; no postcentral areas were detected. At 6 months after baseline, data for second-level analysis were available from only three wait-list survivors, and no activation was detected in the group because of the small number

Table 2. Conners' Parent Rating Scale T scores for the survivors in the fMRI study

Conners' Parent Rating Scale	CRP group ($n = 8$)			Wait-list group ($n = 6$)	
	Pre-CRP	Post-CRP	Follow-up	Pre-CRP	Pre-CRP +6 month
Cognitive problems/inattention	72.6 ± 5.1	65.4 ± 4.7	63.6 ± 5.6	73.3 ± 4.1	67.8 ± 5.9
Hyperactivity	60 ± 3.6	66 ± 6.8	59 ± 6.1	67.8 ± 9.0	63.8 ± 7.3
ADHD	67 ± 3.4	62.9 ± 5.3	59.5 ± 5.4	71.4 ± 5.0	63.6 ± 7.4

Note: Conners' parent rating scale *T* scores, mean = 50, *SD* = 10. The CRP group had significant differences between pre-CRP and follow-up in Cognitive Problems/Inattention ($p = .02$, $d = -0.6$) and in ADHD ($p = .04$, $d = -0.6$). No follow-up behavioral data available for the wait-list control group. No CRP treatment effect was detected, which may reflect limited statistical power with the small sample size.

Table 3. CPT activation of healthy controls

Brain regions in the activation cluster	Cluster size (voxels)	Peak MNI coordinate	T_{max}	Z_{max}
CPT > Fixation				
(L.) inf. occipital (37%), mid. occipital (33%), fusiform (21%), lingual (5%)	772	[−26, −96, 4]	8.4	5.9
(R.) inf. occipital (75%), fusiform (21%)	254	[40, −86, −12]	7.2	5.3
(L. and R.) SMA (84%), mid. Cingulate (12%)	538	[6, 8, 52]	9.0	6.1
(L.) inf. frontal, insula (92%)	66	[−34, 18, 6]	6.5	5.0
(L.) cerebellum: area 6 (54%), crus1 (42%)	608	[−38, −56, −20]	9.4	6.2
(R.) cerebellum: area 6 (60%), crus1 (36%)	456	[36, −60, −24]	9.0	6.1
Fixation > CPT:				
(L. & R.) precuneus (52%), mid. cingulate (12%), cuneus (9%), calcarine (9%), posterior cinguluate (8%), paracentral lobule (3%), lingual (2%)	3000	[2,−56, 32]	8.9	6.0
(R.) postcentral (80%)	294	[56, −8, 32]	8.6	5.9
(L.) postcentral (47%), precentral (10%)	228	[−18, −28, 62]	8.7	6.0
(R.) putamen (40%)	57	[36, −10, 4]	6.5	5.0
Omission (positive)				
(L.) inferior parietal (17%)	113	[−36, −38, 36]	8.5	5.5
Omission (negative)				
(L.) supramarginal (52%), angular (25%), inferior parietal (21%)	108	[−50, 48, 30]	7.8	5.2

Note: Data listed here were obtained by using the following thresholds: cluster extent $k = 50$ voxels ($p = .002$, cluster size corrected $p = .001$) and $T = 5$ (uncorrected $p < .001$, family-wise corrected $p = .48$). With $T = 5$ as a threshold, the cluster level corrected $p = .05$, corresponding to $k = 19$ voxels. The percentage of anatomic area in each cluster was determined by using the Anatomical Automatic Labeling toolbox (AAL) (Tzourio-Mazoyer et al., 2002). Anatomic areas with small percentages in a cluster, corresponding to less than 19 voxels, were not reported. No cluster survived this threshold for Commission and other performance parameters, CCI and RT. With stricter thresholds: voxel height $p = .05$ (family-wise corrected, corresponding to $T = 6.25$) and cluster extent $k = 5$ (uncorrected $p = .12$, corrected $p = .006$), the same anatomic areas, though with a smaller overall cluster size, were identified as being activated or deactivated, except for left insular for "CPT > Fixation", which was replaced with left thalamus. No cluster survived these thresholds for performance parameters. The voxel size was $2 \times 2 \times 2$ mm^3.

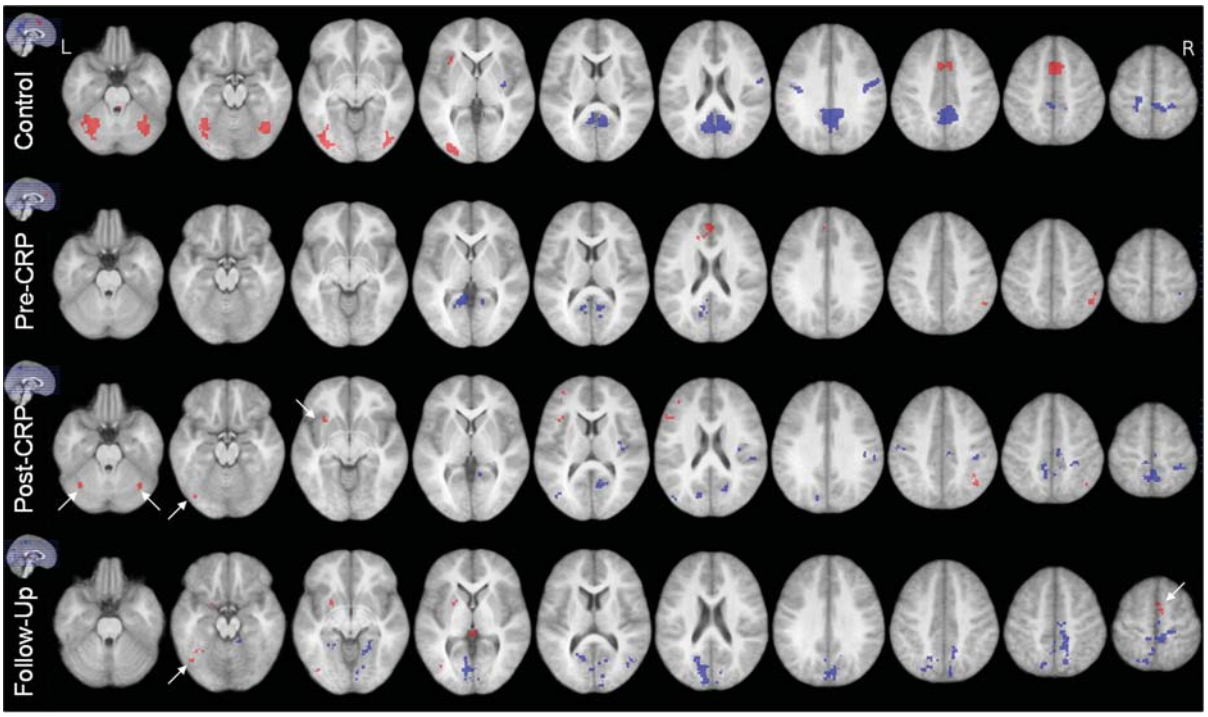

Fig. 1. Group activation for CPT. The images are displayed as left is corresponding to the left hemisphere. Activation (red) and deactivation (blue) were detected when using the following thresholds: cluster extent $k = 50$ voxels ($p = .002$, cluster size corrected $p = .001$) and $T = 5$ (uncorrected $p < .001$, family-wise corrected $p = .48$). The activation and deactivation clusters from the control group constitute the ROIs in ROI analysis. Pre-CRP included nine cancer survivors before CRP treatment (five CRP and four wait-list controls); post-CRP included six cancer survivors (three CRP and three initial wait-list controls); Follow-up included six cancer survivors (all CRP) at 6 months after CRP completion. Arrows point to activation detected in the ROIs after CRP or at follow-up for the survivors.

Table 4. CPT activation of cancer survivors treated with CRP

Brain regions in the cluster	Cluster size (voxels)	Peak MNI Coordinate [X Y Z]	T_{max}	Z_{max}
Pre-CRP: CPT > fixation				
(L.) ant. cingulate (49%), sup. med. frontal (31%)	172	[−4, 46, 24]	11.2	4.6
(R.) inf. parietal (98%)	96	[52, −54, 48]	9.6	4.4
Pre-CRP: fixation > CPT				
(L.) calcarine (39%), precuneus (23%), lingual (20%), cuneus (13%)	380	[−8,−58,18]	14.3	5
(R.) calcarine (62%), lingual (32%),	183	[14, −72, 16]	10.3	4.5
(R.) precentral (100%)	57	[34,−42,64]	8.6	4.2
Post-CRP: CPT > Fixation				
(R.) angular (66%), inf. parietal (34%)	76	[42, −56, 44]	25.8	4.8
(L.) cerebellum: crus 1 (43%), area 6 (32%) fusiform (17%)	87	[−34, −64, −28]	13.7	4.1
(R.) cerebellum: crus 1 (50%), area 6 (35%) fusiform (14%)	78	[38, −64, −26]	11.4	3.9
(L.) mid. frontal (43%), inf. frontal (33%), insular (24%)	220	[−56,22,20]	11.8	4.0
Post-CRP: fixation > CPT				
(R.) calcarine (57%), cuneus (17%), lingual (10%)	175	[12, −66, 10]	18.6	4.5
(L. and R.) precuneus (60%), mid. cingulate (12%), paracentral lobule (12%), (R.) SMA (11%)	705	[2, −46. 62]	14.8	4.2
(L.) sup. occipital (55%), cuneus (40%)	88	[−16,−76, 26]	12.3	4
(L.) mid. occiptial (84%)	113	[−44, −80, 16]	18.5	4.5
(R.) postcentral (66%), supramarginal (26%)	458	[42, −30, 40]	17.9	4.4
(L.) postcentral (95%)	56	[−58. −14, 38]	7.5	3.4
(R.) insula (62%), rolandic_oper (30%)	81	[36, −14, 18]	10.7	3.8
Follow-up: CPT > fixation:				
(L.) inf. occipital (45%), fusiform (23%), mid. occipital (22%), cerebellum_6 (9%)	176	[−42, −76, −2]	31.5	5.0
(L.) putamen (78%), olfactory (15%)	103	[−24, 6, 0]	20.0	4.5
(L.) SMA (85%), (R.) SMA (15%)	60	[2, 0, 66]	8.5	3.6
Follow-up: fixation > CPT				
(L. and R.) cuneus (25%), calcarine (21%), precuneus (15%), lingual (11%), (r.) paracentral lobule (8%), sup. parietal (4%), precentral (1%), postcentral (1%), (l.) sup. occipital (3%)	2047	[14, −52, 52]	19.9	4.5
(R.) mid. temporal (94%)	69	[44, −72, 14]	19.2	4.5
(L.) sup. parietal (52%), precuneus (38%)	276	[−8, −66, 40]	12.8	4.1
(L.) lingual (69%), fusiform (17%)	59	[−20, −46, −6]	12.6	4.0
(R.) lingual (74%), cerebellum_4_5 (14%), fusiform (6%)	112	[24, −50, −6]	11.0	3.9
(R.) SMA (81%)	84	[4, −18, 60]	9.2	3.7

Note: Data listed here were obtained by using the following thresholds: cluster extent $k = 50$ voxels ($p = .002$, cluster-size corrected $p = .001$) and $T = 5$ (uncorrected $p < .001$, family-wise corrected $p = .48$). Pre-CRP included nine cancer survivors before CRP treatment; Post-CRP included six cancer survivors (three from CRP treatment group, three from waiting-list group after CRP treatment *); Follow-up included six cancer survivors in the CRP group at 6 months after completing CRP. The voxel size was $2 \times 2 \times 2$ mm^3.

of participants. At post-CRP, compared with at pre-CRP, the brain activation of the six survivors with CRP involved more of the regions that were activated in the healthy children, such as cerebellum_crus 1, cerebellum_area 6, and fusiform, and left inferior frontal area and insula (Table 3 and Fig. 1). Brain deactivation was detected in more areas of precuneus and the post-central gyrus. At follow-up, inferior occipital, fusiform, and cerebellum_area 6, and the left SMA were activated in the survivors; furthermore, "deactivation" patterns became more similar to those of the healthy controls.

In the healthy control group, omission errors were associated with activation in the left inferior parietal gyrus and inversely associated with activation in the left supramarginal gyrus, left angular gyrus, and the left inferior parietal cortex (Table 3). CCI and reaction time were not associated with any brain region in the healthy controls. No significant association of brain regions and CPT performance parameters was detected in survivors.

ROI Analysis

The ROIs were constructed from activation clusters detected in the second-level group analysis of healthy participants, with the cluster-level threshold (Tables 3 and 5, and Fig. 1). Six activation ROIs—left occipital, right occipital, left inferior frontal, left cerebellum, right cerebellum, and medial pre-frontal (SMA and anterior cingulate) regions—and four deactivation ROIs—left central, right central, putamen, and precuneus—were identified.

When all participants were included in the analysis, the CPT CCI and nAI were significantly associated inversely for all six activation ROIs but not for any of the deactivation ROIs (Table 5 and Fig. 2): left occipital ($r = -.35$, $p = .01$), right occipital

Table 5. ROI results of cancer survivors: normalized AI (nAI) for each ROI cluster and LI for occipital and cerebellum ROIs

ROI	CRP survivor group			Wait-list survivor group		All survivors with CRP*		Healthy control group ($n = 28$)
	Pre-CRP ($n = 5$)	Post-CRP ($n = 3$)	Follow-up ($n = 6$)	Pre-CRP ($n = 4$)	Pre-CRP + 6 month ($n = 2$)	Pre-CRP ($n = 9$)	Post-CRP* ($n = 6$)	
	nAI							AI
L. Occipital	0.5 (0.3, 08)	1 (0.8, 1.3)	0.5 (0.2, 1.0)	0.4 (0.1, 1)	0.6 (0.6, 0.7)	0.5 (0.1, 1)	0.9 (0.3, 1.7)	1769
R. Occipital	0.6 (−0.1, 1.2)	1.3 (0.4, 2)	0.4 (0, 1.1)	0.4 (−0.4, 1)	0.6 (0.3, 0.8)	0.6 (−0.4 1.2)	0.9 (0.3, 2)	524
SMA/cingulate	1.3 (0.5, 1.9)	0.7 (0.4, 1.3)	0.8 (0, 1.0)	0.1 (0, 0.6)	0.6 (0, 1.2)	0.5 (0, 1.9)	0.4 (0, 1.3)	1226
L. inf. front/insula	1.0 (0, 2.5)	1.4 (0.8, 1.5)	0 (0, 0.8)	0.2 (0, 1.3)	−0.5 (−1, 0)	0.3 (0, 2.5)	0.5 (0, 1.5)	136
L. Cerebellum	0.4 (0.1, 1.1)	0.3 (0.3, 0.5)	0.4 (0.1, 1.3)	0.2 (0, 1.1)	0.4 (0.4, 0.5)	0.2 (0, 1,1)	0.4 (0, 0.6)	1269
R. Cerebellum	1 (0.1, 2)	0.6 (0.1, 1)	0.6 (0.1, 1)	0.7 (0, 0.8)	0.6 (0.3, 0.8)	0.7 (0, 1.9)	0.6 (0.1, 1)	1045
L. Central	0.3 (0.2, 1.4)	0.9 (0.1, 2)	0.4 (−0.1, 1.4)	−0.2 (−0.5, 0.3)	0.4 (0.2, 0.6)	0.3 (−0.5, 1.4)	0.9 (0, 2)	−310
R. Central	0.5 (−0.4, 1.2)	0.3 (0.2, 0.6)	0.7 (−0.1, 2.0)	0.1 (−0.7, 0.9)	1.2 (0.9, 1.5)	0.2 (−0.7, 1.2)	0.5 (0, 1.9)	−397
Putamen	0.1 (0, 0.7)	0.4 (−0.1, 1.9)	0 (0, 1.2)	0 (0, 3.4)	0.5 (0.2, 0.7)	0 (0, 3.4)	1.4 (−0.1, 4)	−55
Precuneus	0.6 (0, 1.1)	0.1 (0.1, 0.7)	0.3 (0.2, 0.8)	0.3 (−0.3, 0.8)	0.7 (0.3, 1)	0.4 (−0.2, 1.1)	0.3 (−0, 1)	−4798
	LI							
Occipital	0.5 (0.1, 1.2)	0.4 (0.4, 0.8)	0.6 (0.3, 1)	0.4 (−0.1, 1.6)	0.6 (0.5, 0.7)	0.5(−0.1, 1.6)	0.5 (−0.1, 0.8)	0.5
Cerebellum	0 (−0.7, 0.6)	−0.1 (−0.8, 0.9)	0.1 (−0.3, 0.5)	−0.1 (−0.8, 0.9)	0.2 (0, 0.4)	0(−0.8, 0.9)	0.1 (−0.7, 0.5)	0.1

Note: Results are in median (min, max) format. All survivors with CRP* included nine cancer survivors at pre-CRP (five CRP and four initial wait-list); six cancer survivors at post-CRP (three CRP and three initial wait-list). AI was defined as sum of t values for all voxels with $t > 2$ for a given ROI. nAI was a scaled AI so that the average of the healthy subjects nAI = 1 for the corresponding ROI.

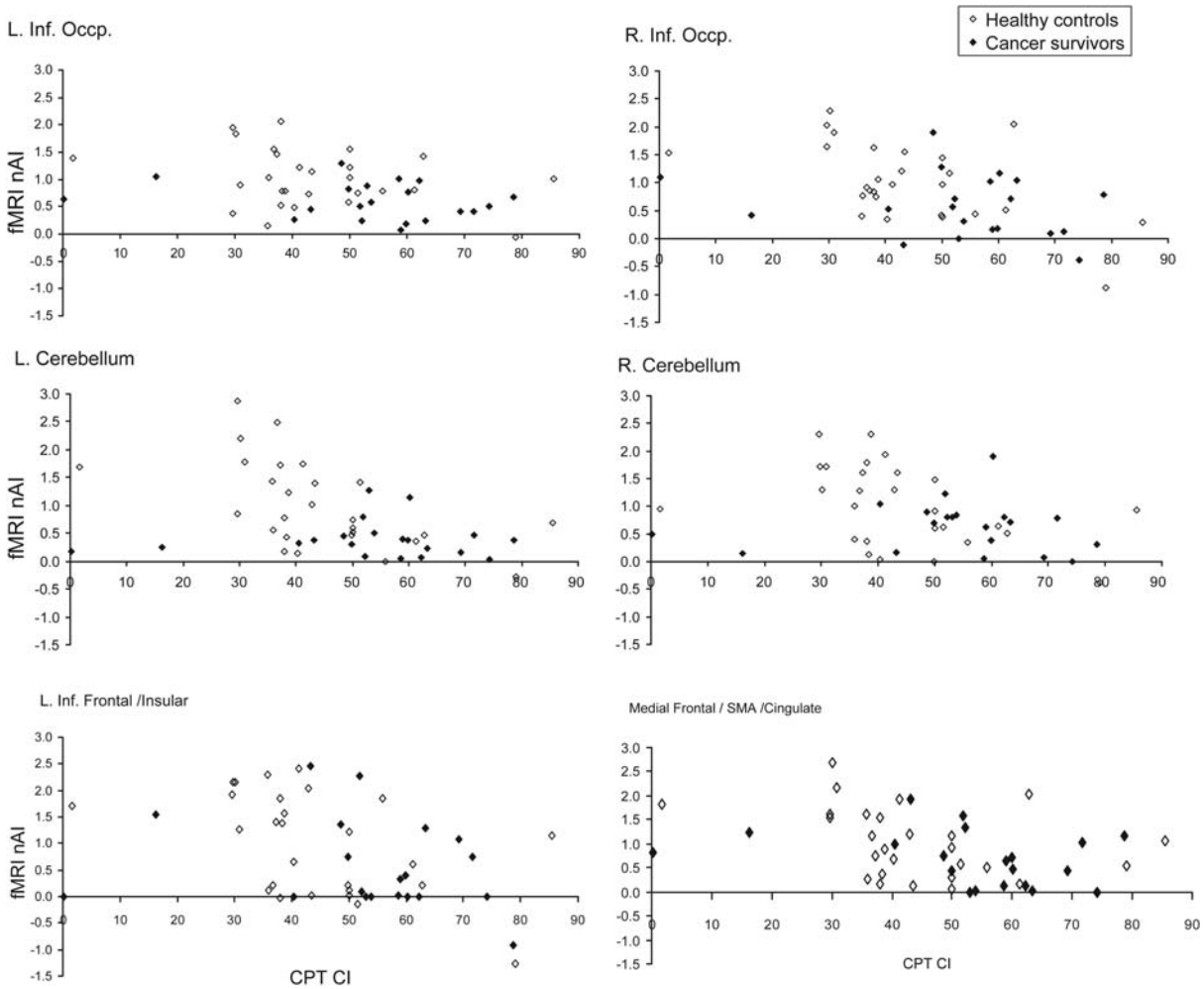

Fig. 2. Association of fMRI nAI and CPT CCI for the Six Activation ROIs.

($r = -.47$, $p < .001$), medial pre-frontal ($r = -.42$, $p = .003$), left inferior frontal ($r = -.43$, $p = .002$), left cerebellum ($r = -.47$, $p < .001$), and right cerebellum ($r = -.37$, $p = .01$).

At pre-CRP, between the 28 healthy controls and 9 survivors (5 in CRP and 4 in wait-list), there were significant differences in nAI at two activation ROIs: left occipital ($p = .003$, $d = -0.35$) and left cerebellum ROI ($p = .01$, $d = -0.41$), and at two deactivation ROIs: right central ($p = .03$, $d = -0.36$) and left central ($p = .015$, $d = -0.42$).

At post-CRP, a significant difference in nAI between healthy controls and six survivors ($p = .04$, $d = -0.36$) with CRP was detected only at the left cerebellum ROI.

At follow-up, between the healthy controls and six CRP group survivors, significant differences in nAI were detected at left occipital ($p = .05$, $d = -0.33$), left inferior frontal ($p = .03$, $d = -0.37$), and left cerebellum ($p = .04$, $d = -0.34$) of the activation ROIs; and at the posterior cingulate ($p = .05$, $d = -0.34$) of the deactivation ROIs.

There was significant left lateralization of activation in the occipital ROI (LI = 0.5 for healthy controls and LI = 0.4–0.6 for cancer survivors; $p < .001$). The LI was not significantly different from zero in the cerebellum for healthy controls or for survivors. There were no significant differences in LIs between healthy controls and either survivor group for any timepoints. The LI did not significantly change over time in either the survivor CRP group or the survivor wait-list group.

Illustrative Case Summaries

To demonstrate brain activation patterns observed in a "non-responder" (no improvement in CCI after CRP) and a "responder" (improved CCI after CRP), imaging and behavioral data for two survivors are summarized here (Table 6).

Table 6. Normalized AI for the activation ROIs, CPT clinical index, and Conners' Parent Report Scale *T* scores for two exemplary CRP participants

	Normalized AI (nAI)						CPT CCI	Conners Parent Rating Scale (*T* score)		
	Left occipital	Right occipital	SMA Cing.	Left insula	Left cerebellum	Right cerebellum		Cogntive problems/ inattention	Hyper-activity	ADHD
Survivor 1										
Pre-CRP	0.51	0.58	1.59	2.27	0.80	1.23	52	72	44	65
Post-CRP	0.83	1.28	0.43	0.76	0.31	0.69	50	55	49	45
Follow-up	0.20	0.18	0.72	0.41	0.38	0.39	60	44	44	42
Survivor 2										
Pre-CRP	0.45	−0.11	1.94	2.45	0.37	0.17	61	57	61	54
Post-CRP	1.04	0.42	1.25	1.54	0.25	0.14	16	84	85	73
Follow-up	0.63	1.10	0.82	0.00	0.17	0.50	0	59	58	53

Note: Mean nAI = 1 for healthy volunteers for each activation ROI; CPT CCI in percentile, a score >50 suggests >50% chance of attention deficits; Conners' parent rating scale *T* scores, mean = 50, *SD* = 10.

Survivor 1 (a "non-responder," first row of Table 1) was a 15-year-old female diagnosed with ALL at age 4.3. Her treatment included chemotherapy and radiation therapy. At pre-CRP neuropsychologic testing, her intellectual skills were assessed as within the average range. Her performance was excellent in the areas of sustained, controlled, selective, and divided attention but poor on the alternating attention. She performed poorly on memory tasks, falling in Extremely Low range on the Wide Range Assessment of Memory and Learning Sentence Memory subtest, and Story Recall on the Children's Memory Scale. She also performed within the Extremely Low range on WISC-III Digit Span subtest. Her CRP sessions focused primarily on improving memory by teaching her to use mnemonic strategies to improve memory. A computerized training module was included to improve mental processing speed and attentional control. Later sessions focused on shifting attention and task set, increasing speed and working memory capacity, and improving memory. Upon completing the CRP and 6-month post-CRP follow-up, her processing speed and working memory improved, as did her attention-shifting skills. She showed dramatic improvement in the areas of mathematics and reading comprehension. Survivor 1 showed no improvement in CPT CCI, but had better Cognitive Problem/Inattention and ADHD scores from parent report after CRP (Table 6). Before remediation, fMRI activation in Survivor 1 (Fig. 3, Table 6) was predominant in the right hemisphere, including visual areas, and was substantially reduced in the medial frontal prefrontal areas. After remediation, there was a relative shift in activation from the right to the left hemisphere, but no increase in medial prefrontal activation and the overall pattern of activation remained abnormal for the CPT task.

Survivor 2 (a "responder," second row of Table 1) was an 11.7-year-old female, diagnosed with ALL at age 2.8. She had low-dose methotrexate chemotherapy but no radiation therapy. At pre-CRP neuropsychologic testing, her WISC-III FSIQ was within the borderline range. She performed well in the areas of sustained and divided attention but experienced difficulties with controlled, selective, and alternating attention. Her pattern of responding suggested a sacrifice of accuracy for speed. Her performance on memory tasks was within the average range except for Story Recall on the Children's Memory Scale, where she was in low average range for immediate recall but extremely impaired for delayed recall. Her CRP focused primarily on improving the speed of target detection and discrimination, while maintaining accuracy of responses. This component of the intervention utilized a combination of visual and auditory tasks. A computerized training module was included to improve mental processing speed and attentional control. Distraction was introduced about halfway through the intervention, and she learned the strategies for resisting distraction, which she applied successfully during selective attention tasks. Overall, she showed improvement on virtually all attention-related tasks, especially with respect to processing speed: her response style became progressively faster, without a speed-accuracy trade-off. Her CPT CCI no longer indicated attention deficits at post-CRP and follow-up, but there was no improvement in parent report (Table 6). Before remediation, fMRI in Survivor 2 (Fig. 4, Table 6) showed a lack of activation in visual areas and strong bilateral anterior frontal activation. After remediation, there was an increase in activation in visual areas, decreased activation in the anterior frontal cortex, and the overall pattern of activation was more like the pattern observed in controls.

Discussion

In the multicenter, clinical trial, the CRP intervention was associated with improved attention by parent report and increased academic achievement with moderate effect sizes. For vigilance measured by the Conner's CPT, all participants showed improved performance between the time of screening and 6 months later, but there were no significant interactions between

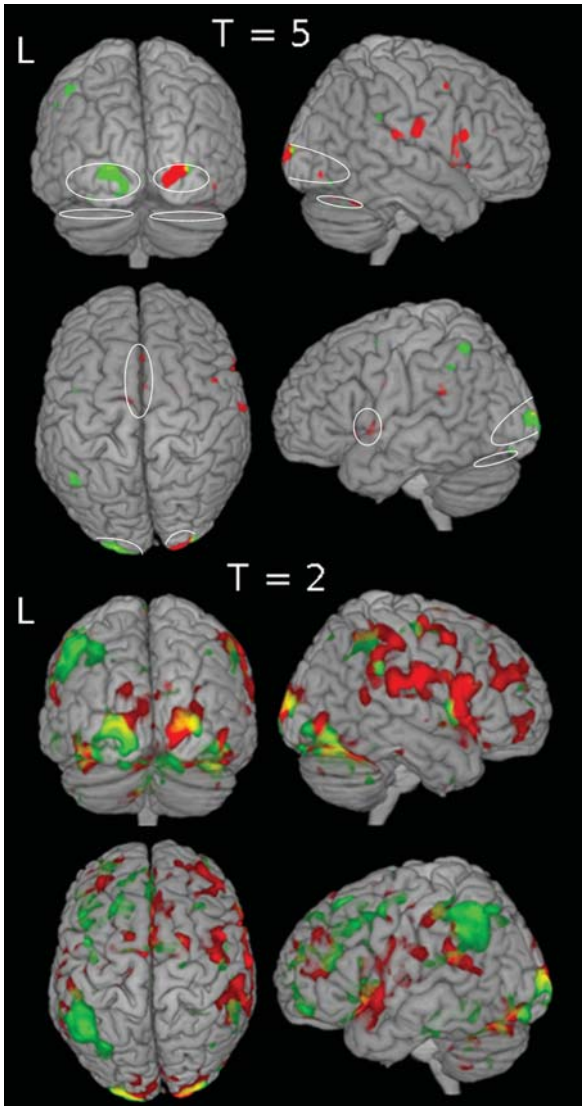

Fig. 3. Pre- and post-CRP brain activation for a non-responder. Pre-CRP (red) and Post-CRP (green) brain activation for the fMRI CPT are shown with thresholds $T = 5$ and $T = 2$. The follow-up (not shown) activation resembles the activation pattern of pre-CRP. Ovals (on the $T = 5$ map) indicate activation ROIs identified from activation map of the healthy volunteers.

the CRP and wait-list control cancer survivor groups and a statistical effect of CRP treatment on the CPT performance was not detected (Butler et al., 2008).

In contrast to the overall multicenter results, for the subset of CRP participants in the optional fMRI study, parent report indicated both CRP and wait-list groups had improvement in attention, but no CRP treatment effect was detected based on the small sample size. The CPT CCI, however, improved only in the CRP group after remediation, and there were significant differences between the CRP and wait-list control groups at the second time point. The CPT CCI changes in the fMRI study were more consistent with the CRP pilot study results (Butler & Copeland, 2002).

Given the multisite design, there are possible differences across sites due to treatment fidelity problems, but this has never been directly tested. Because of the small sample size available in this study, we may lack sufficient statistical power to detect some differences within and between groups. Therefore, important changes in behavior and brain function related to disease, treatment, and remediation may not have been detected in our study. The lack of changes of CPT CCI in the wait-list group may be due to the small sample size or may indeed reflect some CRP treatment effects in the subset of patients who participated in fMRI.

Functional imaging results provided further insight into the CRP treatment effects. The fMRI in healthy children identified large clusters of brain activation similar to those observed in healthy adults (Ogg et al., 2008): left lateralized activation in the

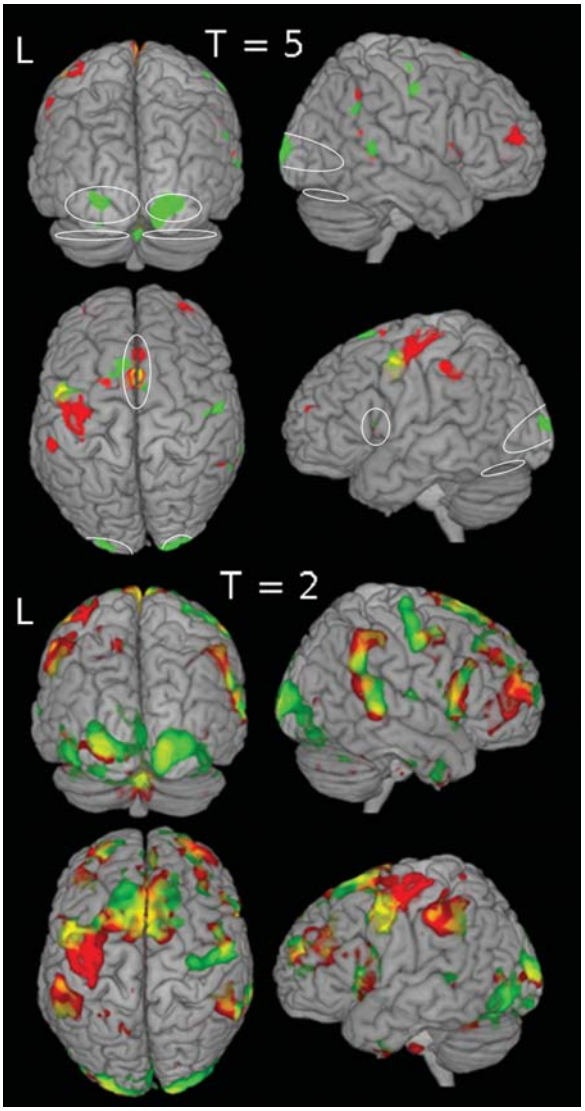

Fig. 4. Pre- and post-CRP brain activation for a responder. Pre-CRP (red) and post-CRP (green) brain activation for the fMRI CPT are shown with thresholds $T = 5$ and $T = 2$. The follow-up (not shown) activation resembles the activation pattern of post-CRP. Ovals (on the $T = 5$ map) indicate activation ROIs identified from activation map of the healthy volunteers.

ventral visual pathway (inferior and middle occipital gyri and fusiform), SMA, left inferior frontal cortex, and bilateral activation in cerebellum (Area 6 and Crus 1). These brain regions are related to visual processing of stimuli, motor planning and control, attentional control, planning and execution, and inhibition control. The significant inverse associations between fMRI AI in these ROIs and the CPT CCI suggest an essential role of this network of brain regions in performing the CPT task. Therefore, disease- or treatment-related changes in these brain regions or their connections could underlie abnormal performance of the task.

As in adults, the ventral visual areas were the most prominently activated areas during the CPT task in the healthy children, and the activation was highly left-lateralized. These left ventral visual areas are associated with object recognition requiring attention (Thoma & Henson, 2011) and are more specialized in visual letter recognition and phonologic decoding (Dietz, Jones, Gareau, Zeffiro, & Eden, 2005), although both left and right extrastriate areas are recruited for such tasks. In contrast, no activation in the extrastriate visual areas was detected in cancer survivors' pre-CRP. After CRP treatment, small bilateral clusters in fusiform areas were detected, and increased activity was detected in left ventral visual areas 6-month later at follow-up in the CRP group. ROI analysis also indicated a significant increase in nAI in the left ventral visual areas in the CRP group from pre- to post-CRP. It is possible that patients were able to better focus on the task and read the letter stimuli after

completion of CRP training. Six months after CRP, fMRI showed still more detectable left ventral visual activation in survivors with remediation. Although overall activation was much lower in the cancer survivors, the relative lateralization of activation in the extrastriate visual areas in healthy controls was similar to that of the cancer survivors at all time points. Thus, despite the diminished BOLD signal in the cancer survivors, the functionally important lateralized activation in the visual system was still detectable in these children. It is possible that the specialization of the ventral visual areas is mostly intact and top-down modulation by attention on extrastriate visual areas (Chawla, Rees, & Friston, 1999) improved after CRP.

Although healthy volunteers had strong bilateral activation in posterior cerebellum regions (i.e., Area 6 and Crus 1), there was no task-related activation in the cerebellum of survivors before CRP treatment. Area 6 and Crus 1 of cerebellum are thought to be involved in language, verbal working memory, spatial tasks, and executive functions (Stoodley & Schmahmann, 2009). At post-CRP and follow-up, activation was again detected in Area 6 and Crus 1 in the cancer survivors. The increase of cerebellum activation may indicate that survivors were engaged and using their brain in a more typical way during the CPT task after receiving the CRP treatment.

There were differences between the activation locations of the medial area in healthy children and those in cancer survivors. In the healthy controls, the activation was in the dorsal region of the prefrontal areas, SMA, and middle cingulate. In the survivors with CRP, the activation areas were mainly in the anterior cingulate at pre-CRP and in SMA at follow-up. SMA and dorsal or rostral parts of the cingulate cortex are thought to be involved in various aspects of attention allocation, motor planning, inhibitory control, error detection; and different sub-area of these areas may be more specifically involved in these processes (Chouinard & Paus, 2006; Petit, Courtney, Ungerleider, & Haxby, 1998; Picard & Strick, 2001; Rushworth, Walton, Kennerley, & Bannerman, 2004; Strick, Dum, & Picard, 1998). In a functional connectivity study, the rostral cingulate area was more connected with prefrontal and language-associated cortex, and the caudal cingulate area was more connected with the sensory cortex (Habas, 2010). These subtle differences of activation location in the medial regions between survivors and healthy controls may thus reflect a range of underlying neural differences, including alterations of functional connectivity, motor planning strategies, attention, and executive functions. Again, 6 months after CRP treatment at follow-up, the medial prefrontal activations in cancer survivors were more similar to those in healthy children.

Together with dorsal anterior cingulate cortex/medial superior frontal cortex, insula/frontal operculum regions are considered as a "core" task-set system (Dosenbach et al., 2006). Detection of activation in the left insula region in the survivors after the CRP treatment suggested that the CRP may help the children engage proper brain regions during cognitive tasks.

The brain areas that were deactivated during the CPT task performance in the healthy controls were consistent with the default mode network (DMN) (Raichle et al., 2001; Buckner, Andrews-Hanna, & Schacter, 2008). The DMN is observed in a variety of cognitive tasks and is also detected in the resting state. This network is involved in baseline brain activities, such as environmental monitoring, internal dialogue, and daydreaming. These baseline activities appear to be suppressed during demanding task periods, and the DMN is deactivated for more demanding tasks (Singh & Fawcett, 2008). The DMN appears to be more active (i.e., less deactivation detected) before an error is made (Eichele et al., 2008). Alterations of the DMN are also associated with various brain disease conditions (Buckner et al., 2008; Broyd et al., 2009). The less robust DMN detected in cancer survivors may mean that survivors were less engaged in the task, have some global alteration of brain function, or fail to appropriately disengage the DMN during task periods resulting in cognitive interference. Again, the changes in the DMN in survivors after CRP treatment and at follow-up may reflect CRP treatment effects.

As illustrated by the data from Survivors 1 and 2, fMRI can detect differences in brain activity at baseline that may be useful for planning cognitive remediation and changes in brain activity after remediation that may help to clarify the effects of intervention. Survivor 1 had essentially no CPT improvement after intervention, potentially because her CRP-targeted memory more than attention. Post-CRP, she had increased activation in the left ventral visual area; however, activations in other ROIs were not detected or even decreased. Her overall brain activation was more left lateralized after CRP, which may reflect a change of task strategies that was associated with effects of CRP that improved her parent rating scale scores. Survivor 2 was an excellent responder to the CRP based on improvement in the CPT CCI. Her pre-CRP fMRI had strong activation at frontal lobes, but little activation at the ventral visual areas. Increased ventral posterior activation and decreased frontal activation post-CRP suggest that her CRP, which focused on increasing capacity in accurate target discrimination and resisting distraction, tuned her brain to activate the proper areas for efficient letter recognition and thus to work in a more organized way typical for the CPT task.

This study was limited by the small sample size of the cancer survivor groups and missing time points across the study. Different treatment regimens for the childhood cancer survivors and different types or locations of tumors for brain tumor survivors could have contributed large variance to the fMRI data. Thus, the power to detect activation in the survivors and to detect the CRP treatment effects was limited. Furthermore, the CRP program was individualized; and the group results only reflect common components. Nevertheless, intervention-related changes of activation in brain regions supporting CPT performance were observed. The ROI analysis supplemented the stricter second-level random effect analysis and revealed

additional evidence that the imaging results were associated with clinical measures. Finally, imaging results in individual patients showed meaningful inter-subject differences at baseline and intra-subject changes after intervention.

In conclusion, CRP treatment in cancer survivors may be associated with changes in cortical activity, which can be evaluated by using fMRI. A better understanding of these changes in brain activation patterns can be used to design and evaluate behavioral and pharmacologic interventions to treat cognitive deficits. Data from fMRI may help identify patients most likely to experience a response on the basis of altered networks. Ultimately, insight into functional alterations may help guide efforts to improve cancer treatment protocols involving CNS therapy to minimize long-term damage to important functional areas of the brain.

Funding

This work was supported in part by the Pediatric Brain Tumor Foundation [PBTFUS to R.J.O.], National Institutes of Health [HD049888 to R.J.O., RO1 CA83936 to R.W.B.], National Cancer Institute (Comprehensive Cancer Center Support Grant P30CA21765), and American Lebanese Syrian Associated Charities.

Conflict of Interest

None declared.

References

American Cancer Society. (2011). *Cancer facts and figures 2011*. Retrieved October 11, 2012 from http://www.cancer.org/Research/CancerFactsFigures/CancerFactsFigures/cancer-facts-figures-2011.

Battle, J. (1992). *Culture-free self-esteem inventories* (2nd ed.). Austin, TX: PRO-ED.

Brouwers, P., & Poplack, D. (1990). Memory and learning sequelae in long-term survivors of acute lymphoblastic leukemia: Association with attention deficits. *Am. J. Pediatr. Hematol. Oncol.*, *12*, 174–181.

Brouwers, P., Riccardi, R., Poplack, D., & Fedio, P. (1984). Attentional deficits in long-term survivors of childhood acute lymphoblastic leukemia (ALL). *J. Clin. Neuropsychol.*, *6*, 325–336.

Broyd, S. J., Demanuele, C., Debener, S., Helps, S. K., James, C. J., & Sonuga-Barke, E. J. (2009). Default-mode brain dysfunction in mental disorders: A systematic review. *Neurosci. Biobehav. Rev.*, *33*, 279–296.

Buckner, R. L., Andrews-Hanna, J. R., & Schacter, D. L. (2008). The brain's default network: Anatomy, function, and relevance to disease. *Ann. N. Y. Acad. Sci.*, *1124*, 1–38.

Butler, R. W., & Copeland, D. R. (2002). Attentional processes and their remediation in children treated for cancer: A literature review and the development of a therapeutic approach. *J. Int. Neuropsychol. Soc.*, *8*, 115–124.

Butler, R. W., Copeland, D. R., Fairclough, D. L., Mulhern, R. K., Katz, E. R., Kazak, A. E., et al. (2008). A multicenter, randomized clinical trial of a cognitive remediation program for childhood survivors of a pediatric malignancy. *J. Consult Clin. Psychol.*, *76*, 367–378.

Butler, R. W., & Haser, J. K. (2006). Neurocognitive effects of treatment for childhood cancer. *Ment. Retard. Dev. Disabil. Res. Rev.*, *12*, 184–191.

Carey, M. E., Haut, M. W., Reminger, S. L., Hutter, J. J., Theilmann, R., & Kaemingk, K. L. (2008). Reduced frontal white matter volume in long-term childhood leukemia survivors: a voxel-based morphometry study. *Am. J. Neuroradiol.*, *29*, 792–797.

Chawla, D., Rees, G., & Friston, K. J. (1999). The physiological basis of attentional modulation in extrastriate visual areas. *Nat Neurosci*, *2*, 671–676.

Chouinard, P. A., & Paus, T. (2006). The primary motor and premotor areas of the human cerebral cortex. *Neuroscientist.*, *12*, 143–152.

Cohen, M. (1997). Children's memory scale. San Antonio, TX: Psychological Corporation.

Conklin, H. M., Khan, R. B., Reddick, W. E., Helton, S., Brown, R., Howard, S. C., et al. (2007). Acute neurocognitive response to methylphenidate among survivors of childhood cancer: a randomized, double-blind, cross-over trial. *J. Pediatr. Psychol.*, *32*, 1127–1139.

Conklin, H. M., Li, C., Xiong, X., Ogg, R. J., & Merchant, T. E. (2008). Predicting change in academic abilities after conformal radiation therapy for localized ependymoma. *J. Clin. Oncol.*, *26*, 3965–3970.

Conners, C. K. (1992). Conners' continuous performance test. Toronto: Multi-Health System, Inc.

Conners, C. K. (1997). Conners' rating scales—Revised. North Tonawanda, NY: Multi-Health Systems, Inc.

Dietz, N. A., Jones, K. M., Gareau, L., Zeffiro, T. A., & Eden, G. F. (2005). Phonological decoding involves left posterior fusiform gyrus. *Human Brain Mapping*, *26*, 81–93.

Dosenbach, N. U., Visscher, K. M., Palmer, E. D., Miezin, F. M., Wenger, K. K., & Petersen, S.E. (2006). A core system for the implementation of task sets. *Neuron*, *50*, 799–812.

Dunn, L. M., & Markwardt, F.C. (1970). *Peabody Individual Achievement Test— Revised*. Circle Pines, MN: American Guidance Services.

Eichele, T., Debener, S., Calhoun, V. D., Specht, K., Engel, A. K., Hugdahl, K., et al. (2008). Prediction of human errors by maladaptive changes in event-related brain networks. *Proc. Natl. Acad. Sci. USA*, *105*, 6173–6178.

Golden, C. J. (1978). *Stroop Color and Word Test*. Chicago: Stoelting.

Habas, C. (2010). Functional connectivity of the human rostral and caudal cingulate motor areas in the brain resting state at 3T. *Neuroradiology*, *52*, 47–59.

Lezak, M., Howieson, D., & Loring, D. (2004). *Neuropsychological assessment*. New York: Oxford University Press.

Liu, T. T. (2004). Efficiency, power, and entropy in event-related fMRI with multiple trial types. Part II: Design of experiments. *Neuroimage.*, *21*, 401–413.

Merchant, T. E., Conklin, H. M., Wu, S., Lustig, R. H., & Xiong, X. (2009). Late effects of conformal radiation therapy for pediatric patients with low-grade glioma: Prospective evaluation of cognitive, endocrine, and hearing deficits. *J. Clin. Oncol.*, *27*, 3691–3697.

Merchant, T. E., Happersett, L., Finlay, J. L., & Leibel, S. A. (1999). Preliminary results of conformal radiation therapy for medulloblastoma. *Neuro. Oncol.*, *1*, 177–187.

Mulhern, R. K., Merchant, T. E., Gajjar, A., Reddick, W. E., & Kun, L. E. (2004). Late neurocognitive sequelae in survivors of brain tumours in childhood. *Lancet Oncol.*, *5*, 399–408.

Mulhern, R. K., Palmer, S. L., Reddick, W. E., Glass, J. O., Kun, L. E., Taylor, J., et al. (2001). Risks of young age for selected neurocognitive deficits in medulloblastoma are associated with white matter loss. *J. Clin. Oncol.*, *19*, 472–479.

Ogg, R. J., Zou, P., Allen, D. N., Hutchins, S. B., Dutkiewicz, R. M., & Mulhern, R. K. (2008). Neural correlates of a clinical continuous performance test. *Magn Reson. Imaging*, *26*, 504–512.

Palmer, S. L., Goloubeva, O., Reddick, W. E., Glass, J. O., Gajjar, A., Kun, L., et al. (2001). Patterns of intellectual development among survivors of pediatric medulloblastoma: a longitudinal analysis. *J. Clin. Oncol.*, *19*, 2302–2308.

Palmer, S. L., Reddick, W. E., & Gajjar, A. (2007). Understanding the cognitive impact on children who are treated for medulloblastoma. *J. Pediatr. Psychol.*, *32*, 1040–1049.

Petit, L., Courtney, S. M., Ungerleider, L. G., & Haxby, J. V. (1998). Sustained activity in the medial wall during working memory delays. *J. Neurosci.*, *18*, 9429–9437.

Picard, N., & Strick, P. L. (2001). Imaging the premotor areas. *Curr. Opin. Neurobiol.*, *11*, 663–672.

Raichle, M. E., MacLeod, A. M., Snyder, A. Z., Powers, W. J., Gusnard, D. A., & Shulman, G. L. (2001). A default mode of brain function. *Proc. Natl. Acad. Sci. USA*, *98*, 676–682.

Reddick, W. E., Glass, J. O., Johnson, D. P., Laningham, F. H., & Pui, C. H. (2009). Voxel-based analysis of T2 hyperintensities in white matter during treatment of childhood leukemia. *AJNR Am. J. Neuroradiol.*, *30*, 1947–1954.

Reddick, W. E., Russell, J. M., Glass, J. O., Xiong, X., Mulhern, R. K., Langston, J. W., et al. (2000). Subtle white matter volume differences in children treated for medulloblastoma with conventional or reduced dose craniospinal irradiation. *Magn Reson. Imaging*, *18*, 787–793.

Reitan, R. (1969). *Manual for administration of neuropsychological test batteries on adults and children.* Bloomington: Indiana University Press.

Rey, A. (1964). *L'examen clinique en psychologie [Clinical tests in psychology]*. Paris: Presses universitaire de France.

Robinson, K.E., Livesay, K.L., Campbell, L.K., Scaduto, M., Cannistraci, C.J., Anderson, A.W., et al. (2010). Working memory in survivors of childhood acute lymphocytic leukemia: functional neuroimaging analyses. *Pediatr. Blood Cancer*, *54*, 585–590.

Rushworth, M. F., Walton, M. E., Kennerley, S. W., & Bannerman, D. M. (2004). Action sets and decisions in the medial frontal cortex. *Trends Cogn Sci.*, *8*, 410–417.

Schmahmann, J. D., Doyon, J., McDonald, D., Holmes, C., Lavoie, K., Hurwitz, A. S., et al. (1999). Three-dimensional MRI atlas of the human cerebellum in proportional stereotaxic space. *Neuroimage.*, *10*, 233–260.

Schretlen, D. (1997). *Brief Test of Attention.* Odessa, FL: Psychological Assessment Resources.

Sheslow, D., & Adams, W. (1990). *Wide Range Assessment of Memory and Learning.* Wilmington, DE: Jastak Associates.

Singh, K. D., & Fawcett, I. P. (2008). Transient and linearly graded deactivation of the human default-mode network by a visual detection task. *Neuroimage.*, *41*, 100–112.

Stoodley, C. J., & Schmahmann, J. D. (2009). Functional topography in the human cerebellum: A meta-analysis of neuroimaging studies. *Neuroimage.*, *44*, 489–501.

Strick, P. L., Dum, R. P., & Picard, N. (1998). Motor areas on the medial wall of the hemisphere. *Novartis. Found. Symp.*, *218*, 64–75.

Talairach, J., & Tournoux, P. (1998). *Co-planar sterotaxic atlas of the human brain*. New York: Thieme Medical.

Thoma, V., & Henson, R. N. (2011). Object representations in ventral and dorsal visual streams: fMRI repetition effects depend on attention and part-whole configuration. *Neuroimage*., *57*, 513–525.

Thompson, S. J., Leigh, L., Christensen, R., Xiong, X., Kun, L. E., Heideman, R. L., et al. (2001). Immediate neurocognitive effects of methylphenidate on learning-impaired survivors of childhood cancer. *J. Clin. Oncol.*, *19*, 1802–1808.

Tzourio-Mazoyer, N., Landeau, B., Papathanassiou, D., Crivello, F., Etard, O., Delcroix, N., et al. (2002). Automated anatomical labeling of activations in SPM using a macroscopic anatomical parcellation of the MNI MRI single-subject brain. *Neuroimage.*, *15*, 273–289.

Wechsler, D. (1991). *Wechsler Intelligence Scale for Children* (3rd ed.). San Antonio, TX: Psychological Corporation.

Wei, X., Yoo, S. S., Dickey, C. C., Zou, K. H., Guttmann, C. R., & Panych, L. P. (2004). Functional MRI of auditory verbal working memory: Long-term reproducibility analysis. *Neuroimage.*, *21*, 1000–1008.

Wilkinson, G.S. (1993). *The Wide Range Achievement Test* (3rd ed.). Wilmington, DE: Wide Range.

Woodcock, R.W., & Johnson, M. B. (1989). *Woodcock–Johnson Tests of Achievement*. Itasca, IL: Riverside.

Zhang, Y., Zou, P., Mulhern, R. K., Butler, R. W., Laningham, F. H., & Ogg, R. J. (2008). Brain structural abnormalities in survivors of pediatric posterior fossa brain tumors: A voxel-based morphometry study using free-form deformation. *Neuroimage.*, *42*, 218–229.

Zou, P., Mulhern, R. K., Butler, R. W., Li, C. S., Langston, J. W., & Ogg, R. J. (2005). BOLD responses to visual stimulation in survivors of childhood cancer. *Neuroimage.*, *24*, 61–69.

Zou, P., Phillips, N., Zhang, Y., Mulhern, R., Merchant, T., Gajjar, A., et al. (2005). BOLD responses in pediatric brain tumor patients during treatment. *Proc. Intl. Soc. Magn. Reson. Med.*, *13*, 441.